Volume 278, number 1, 9–11 FEBS 09280 January 1991

ADONIS 001457939100092J

Solution conformation of endothelin, a potent vaso-constricting bicyclic peptide

A combined use of ^1H NMR spectroscopy and distance geometry calculations

Sharon Munro[1], David Craik[1], David McConville[1], Jon Hall[2], Mark Searle[1], Wendy Bicknell[3], Denis Scanlon[4] and Chris Chandler[4]

[1]*School of Pharmaceutical Chemistry, Victorian College of Pharmacy Ltd, 381 Royal Parade, Parkville, Victoria 3052,* [2]*NSITC, Swinburne Ltd, Hawthorn,* [3]*NMR Facility, Peter MacCallum Cancer Institute, Melbourne and* [4]*Auspep Pty Ltd, Parkville, Australia*

Received 18 October 1990

The solution structure of endothelin-1, a newly discovered potent bicyclic peptide vaso-constrictor agent, has been investigated using ^1H NMR conformational constraints and distance geometry calculations. The conformation is constrained by two disulphide bridges between Cys^1-Cys^{15} and Cys^3-Cys^{11} but the NMR data and computed conformers show additional helical structure between residues Leu^8 and Cys^{11}. Our results are compared with previous conflicting reports on the solution conformation of this peptide

Endothelin; Vaso-active peptide; Distance geometry; ^1H NMR; Three-dimensional conformation

1. INTRODUCTION

The endothelins are a newly discovered mammalian family of biologically active peptides with potent vaso-constrictor properties, originally identified in the culture supernatant of porcine aortic endothelial cells [1]. Endothelin-1 (ET-1), the first member of this family, is a 21 amino-acid peptide whose structure is constrained by two disulphide bridges between residues 1–15 and 3–11 (see Fig. 1). Structure–activity studies have shown that deletion of Trp^{21} results in a decrease in the constrictor response of endothelin by approximately three orders of magnitude, while cleavage of the two disulphide linkages reduces the potency by two orders of magnitude [2]. It is, therefore, of interest to establish the relationship between the primary amino acid sequence and the 3D conformation of ET-1, which may be important for its biological activity.

Two recent reports have outlined the assignment and 3D structure determination of endothelin in d_6-DMSO [3,4]. It is interesting that not only the fingerprint regions of the NOESY spectra shown in these studies are quite different, but also that the derived 3D structures of ET-1 differ significantly. For example, a chemical shift difference of 0.4 ppm for Ser^4 H_N in the two reports is unlikely to be attributable to the small temperature difference between these two studies of only 3°C.

Correspondence address: S. Munro, School of Pharmaceutical Chemistry, Victorian College of Pharmacy Ltd, 381 Royal Parade, Parkville, Victoria 3052, Australia

In the present study we have synthesized a sample of ET-1 with potent biological activity in a pig coronary arterial ring contraction assay [1] and have examined its ^1H NMR spectrum in d_6-DMSO. Following the sequence-specific assignment of the NMR spectrum of the peptide, a family of 3D structures of ET-1 is proposed from the combined use of 2D NOE constraints and distance geometry calculations. We then compare our data to that reported in the two earlier studies.

2. MATERIALS AND METHODS

The peptide was synthesized by solid-phase tBoc chemistry on an ABI 430A peptide synthesizer using automatic 'double-coupling' protocols. The side-chain protecting groups employed were as follows: benzyloxymethyl (Bom) for histidine, 4-methylbenzyl (4MeBzl) for cysteine, 2-bromobenzyloxycarbonyl (BrZ) for tyrosine, 2-chlorobenzyloxycarbonyl (ClZ) for lysine, benzyl (Bzl) for glutamic acid, aspartic acid and serine. The indole ring of tryptophan was not protected. To prevent alkylation of tryptophan during the tBoc deprotection step of the synthesis, 0.1% (w/v) indole was dissolved in the trifluoroacetic acid (TFA) as a scavenger.

On completion of synthesis, the peptide was cleaved from the resin

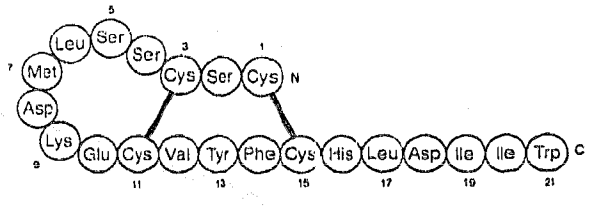

Fig. 1. Amino acid sequence of endothelin-1 (human, porcine, rat, canine).

by treatment with liquid HF/cresol (90:10) for 2 h at −5°C. The peptide resin was washed with cold diethyl ether and then the peptide was extracted into 50% CH_3CN/H_2O (0.1% TFA). This extract was freeze-dried and then resuspended in 25 mM NH_4HCO_3 (pH 8.0; 0.3 mg/ml). The solution was tested with Ellmans reagent for the presence of free sulphydryl groups and then stirred for 24 h at room temperature. No free sulphydryl groups could be detected after this time period. The bicarbonate solution was freeze-dried and the crude endothelin purified to homogeneity by reverse-phase HPLC on a Waters μ-Bondapak preparative reversed-phase column (19 × 150 mm). The yield was approximately 0.5% from the initial loading on the resin at the commencement of synthesis. The peptide was found to have potent biological activity in a pig coronary arterial ring contraction assay, consistent with that previously reported by Yanagisawa et al. [1].

^{1}H NMR spectra were collected at 400 MHz on a Varian VXR400 WB spectrometer and the data processed on a Sun 3/50 data station, both of the Peter MacCallum Cancer Institute NMR Facility. Pure absorption, phase-sensitive DQF-COSY, NOESY and HOHAHA spectra were recorded at 35°C using the hypercomplex method of data collection [5,6] with the carrier frequency placed at the centre of the spectrum. A spectral width of 4000 Hz was employed in all cases with a relaxation delay of 1.5 s incorporated into each sequence. DQF-COSY and 50, 100, 200 and 300 ms NOESY spectra were acquired as 2048 points in t_2 for each of 2 × 400–512 t_1 increments and the data set zero-filled to a 4096 × 2048 data matrix prior to Fourier transformation. Sine-bell and/or shifted sine-bell apodization functions were applied. The 2D HOHAHA spectrum was obtained with the spectrometer configured in the inverse-mode using an MLEV-17 [7,8] mixing scheme with a spin-locking period of 67 ms. In this case 1024 points were collected in t_2 for 2 × 400 t_1 increments. The data set was zero-filled to 1024 points in t_1 prior to Fourier transformation and processed with mild squared-gaussian window functions with a small exponential line broadening component of 0.1 Hz. All data sets were typically acquired in 16–24 h.

Distance geometry calculations were performed on a Vax 11/750 computer, using the DISGEO [9] program. Graphical representation and RMSD analysis were carried out on a Silicon Graphics 4D/70 GT workstation, using the INSIGHT software [10].

3. RESULTS

Assignment [11,12] of the ^{1}H NMR spectrum of ET-1 proceeded by first defining individual amino acid spin systems by a combined analysis of DQF-COSY and HOHAHA spectra. Spin systems were then connected by means of sequential ($N_i - N_{i+1}$ $\alpha_i - N_{i+1}$ $\beta_i - N_{i+1}$) NOEs and equated with unique portions of the primary sequence. By this method it was possible to assign each observed spin system to a unique point in the sequence of ET-1. Fig. 2 shows the $H_\alpha - H_N$ region of a NOESY spectrum for ET-1 (mixing time of 100 ms). The sequential connectivities, together with residue numbers, are marked on the spectrum. The chemical shift data are presented in Table I.

Proton–proton distance constraints were obtained from the analysis of cross-peak intensities of NOESY spectra with mixing times of 50–300 ms. The NOEs were classified into four groups according to their relative intensities, with upper distance bounds cor-

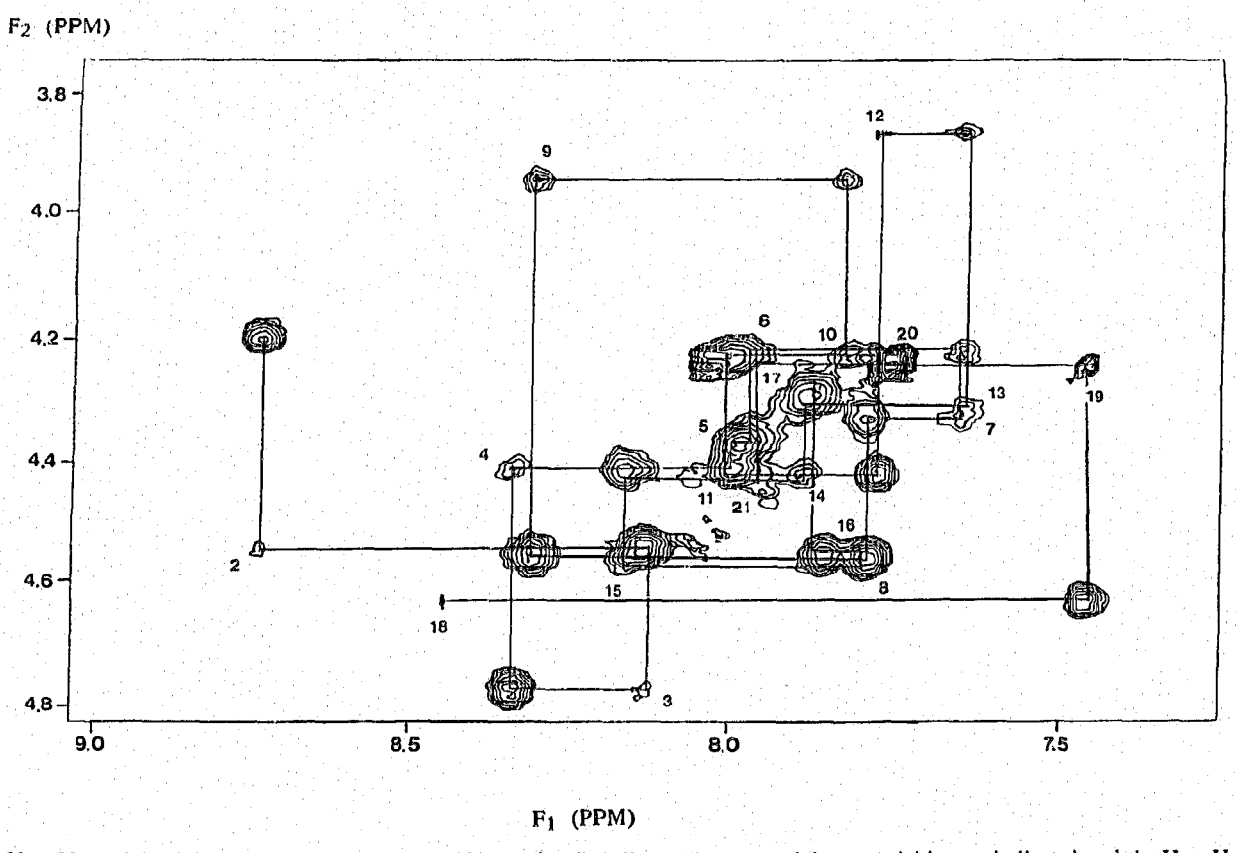

Fig. 2. $H_\alpha - H_N$ region of the NOESY spectrum ($\tau \approx 100$ ms) of endothelin-1. The sequential connectivities are indicated and the $H_\alpha - H_N$ intra-residue cross-peaks labelled.

Table I

Chemical shifts[a] of ET-1 (ppm) in d_6-DMSO at 35°C

Residue	NH	α-CH	β-CH	Others
Cys^1		4.18	3.00, 3.12	
Ser^2	8.78	4.53	3.60	
Cys^3	8.18	4.75	2.83, 3.14	
Ser^4	8.39	4.42	3.58, 3.68	
Ser^5	8.04	4.35	3.56, 3.74	
Leu^6	8.01	4.20	1.48	γH, 1.93; δCH_3, 0.85
Met^7	7.66	4.31	1.81, 1.99	γH, 2.40, 2.56; εH, 2.07
Asp^8	7.82	4.54	2.71, 2.91	
Lys^9	8.35	3.94	1.73	γH, 1.34; δH, 1.54; εH, 2.77 ϵNH_2, 7.70
Glu^{10}	7.85	4.20	1.91, 2.01	γH, 2.35
Cys^{11}	8.04	4.40	2.94, 3.03	
Val^{12}	7.80	3.85	1.94	γCH_3, 0.74, 0.76
Tyr^{13}	7.68	4.26	2.70, 2.78	ring: 2, 6- 6.83; 3, 5- 6.57
Phe^{14}	7.93	4.40	2.92	ring: 2, 6- 7.28; 3, 5- 7.20; 4- 7.29
Cys^{15}	8.20	4.57	2.96	3.14
His^{16}	7.83	4.50	2.95, 3.10	ring: unassigned
Leu^{17}	7.89	4.26	1.49	γH, 1.63; δCH_3, 0.86
Asp^{18}	8.45	4.63	2.46, 2.71	
Ile^{19}	7.46	4.24	1.66	γH, 0.96, 1.34; γCH_3, 0.76; δCH_3, 0.76
Ile^{20}	7.77	4.23	1.69	γH, 1.04, 1.41; γCH_3, 0.81; δCH_3, 0.80
Trp^{21}	8.06	4.50	2.94, 3.03	ring: 4H- 7.50; 5H- 7.00; 6H, 7H- 7.32 2H and NH unassigned

[a]Chemical shift measurements are from plots with d_6-DMSO at 2.45 ppm and H_2O at 3.36 ppm

responding to 2.5, 3.0, 3.5 and 4.0 Å. Covalent constraints limit the intra-residue H_α-H_N distances to the range 2.16 Å < d < 2.85 Å, although the NOE data did not show any H_α-H_N distances to be less than 2.6 Å. For intra-residue distances between amide and Cα-protons, additional constraints were derived, in some cases, from spin-spin coupling constants. In the case of J_{HN} values > 8.0 Hz, lower bound and upper bound distance constraints for corresponding $dH_\alpha - H_N$ values were set to 2.8 Å and 2.9 Å, respectively. The geometrical constraints of the two disulphide bridges were also included in the DISGEO input. In total 61 intra-residue, 45 sequential and 11 medium- and long-range NOE-derived distance constraints were used as input bounds for the distance geometry calculations. A summary of the observed NOE connectivities is presented in Fig. 3. From an initial set of 10 structures (randomly generated), a final set of 7 conformers converged within DISGEO. This family of structures is presented in Fig. 4, where only the peptide backbone is shown for clarity. Although all distance constraints are satisfied simultaneously in any individual structure, we are unable to rule out the possibility of multiple conformers using this approach. The 4 cysteine residues have been superimposed as the reference frame in this representation, with the greatest RMSD over the 4 cysteine backbones being 2.7 Å.

Only the NHs of Ser^2 and Ile^{19} were sufficiently well resolved for their temperature coefficients to be determined and these were 4.76 ppm/1000°C and 3.76 ppm/1000°C, respectively. The data for Ile^{19} suggest some degree of protection from the solvent.

4. DISCUSSION

From the DISGEO structures in Fig. 4 it can be seen that although the two disulphide bridges impose considerable conformational constraints on ET-1, additional structural features are apparent in the computed conformers with the overall appearance of the molecule being somewhat planar in nature. The 3D structure through the Cys^1–Ser^5 segment of the polypeptide is well defined from the NOE data, with a similar conformation observed in each of the seven structures. Intense $H_\alpha - H_N$ peaks are indicative of the presence of a β-sheet type structure, although from the temperature coefficient for Ser^2 NH it would appear that this amide proton is not involved in any hydrogen bonding within this conformation.

In the segment Leu^6–Cys^{11}, the $H_\alpha - H_N$ cross-peak intensities are observed to decrease while those for

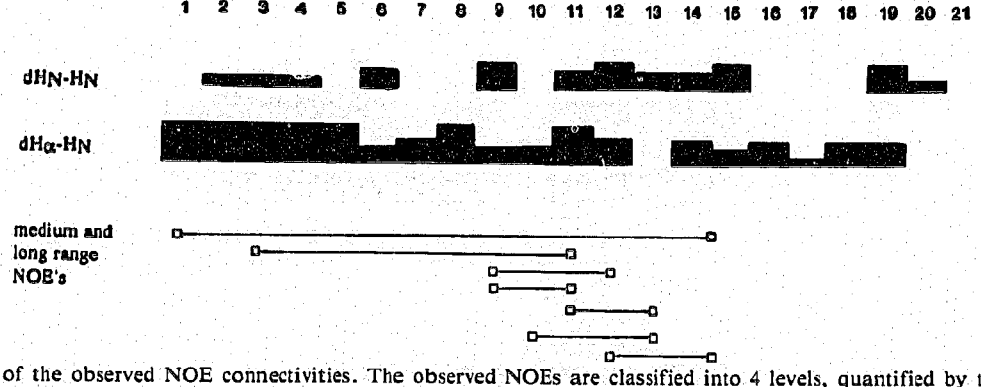

Fig. 3. Summary of the observed NOE connectivities. The observed NOEs are classified into 4 levels, quantified by the height of the bars. Medium- and long-range connectivities are indicated (two NOEs were detected between C^{11}–Y^{13}, three between Y^{13}–E^{10} and two between V^{12}–C^{15}.

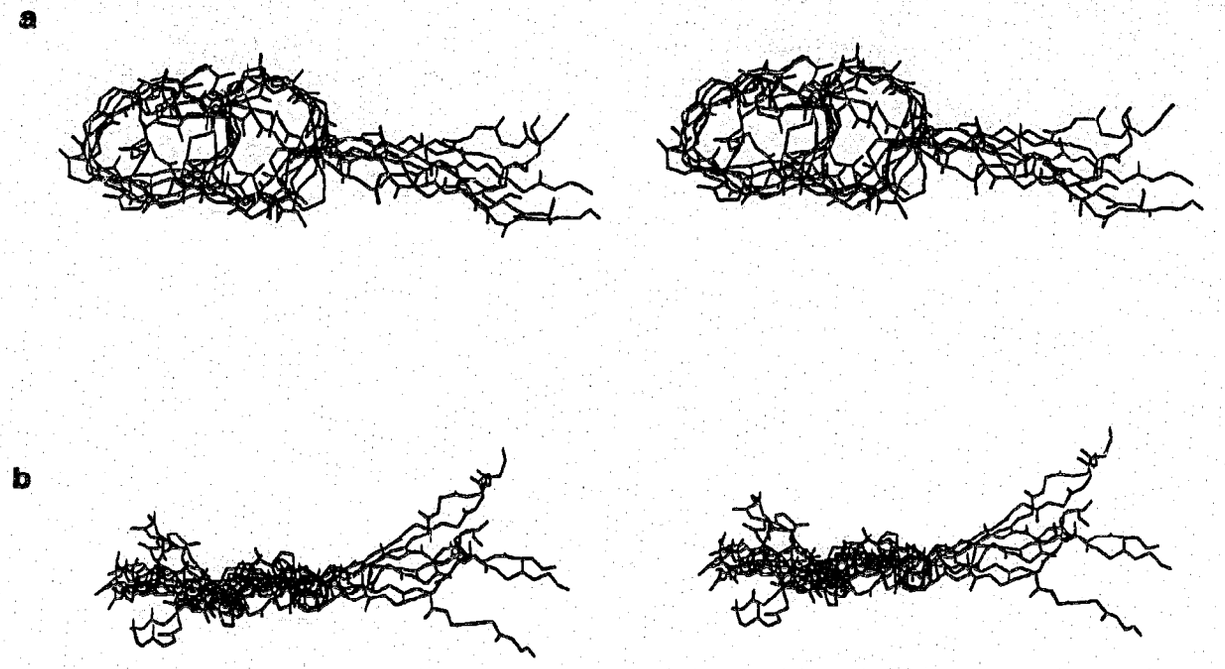

Fig. 4. Stereoview of 7 DISGEO-generated structures (showing only the backbones) of endothelin-1. (a) shows the 7 structures looking down on the two disulphide bridges, whilst (b) shows the same structures rotated 90° on the x-axis.

$H_N - H_N$ become stronger, indicative of an increase in the helical nature of the structure in this region [11]. This structural motif is well represented in the family of computed conformers illustrated in Fig. 4. Moreover, the observation of a cross-peak between H_α of Lys^9 and H_β of Val^{12} indicates that the helical structure in this segment of the polypeptide encompasses the disulphide bridge between Cys^3–Cys^{11}. From the observed NOEs however, the structure present does not appear to be that of a regular α-helix. The 7 DISGEO conformers all contain this structural feature, although some degree of disorder is found for residues flanking the Leu^6–Cys^{11} segment of the polypeptide. The conformation of the sequence Cys^{11}–Cys^{15} is also well-defined in each of the generated structures, which is to be expected as this region of ET-1 has to accommodate the two disulphide bridges.

The conformation of the C-terminal peptide segment is not as well defined by the NOE data. Neither do we observe long-range NOEs between the tail and the main body of ET-1 indicative of a folded conformation. With the exception of a weak sequential NOE between Leu^{17} and Asp^{18}, the NOE data are consistent with an extended random coil conformation for the polypeptide tail, contrary to the findings reported by Saudek et al. [4], but consistent with the results reported by Endo et al. [3].

Several NMR differences are apparent in the two previous reports, particularly for residues 4–11, despite the purity and homogeneity of both samples being checked by HPLC and amino acid analysis. A comparison of the chemical shift data for the H_α and H_N protons with the current work is given in Fig. 5. There are also anomalies between the observed NOEs, and

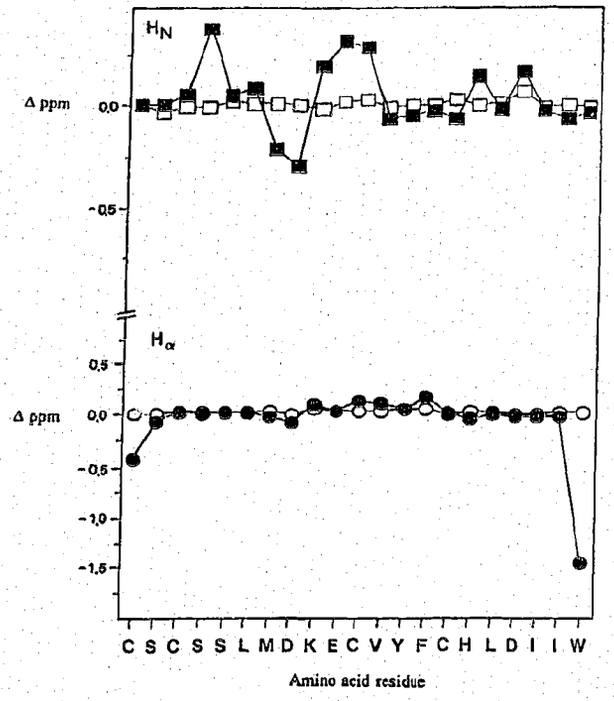

Fig. 5. Difference in reported H_N (top panel) and H_α (lower panel) chemical shifts in this study and those of Endo et al. ([3]; □ and ○) and Saudek et al. ([4]; ■ and ●).

hence derived tertiary structures for endothelin-1, reported in the two previous studies. Although we have not observed as many NOEs as either Endo et al. [3] or Saudek et al. [4] (presumably due to the lower field instrument used in this study compared to the other two reports), all of the medium- and long-range connectivities observed by Endo et al. [3] have been observed in the current study, together with an additional connectivity between Lys^9–Cys^{11}. Consequently, the tertiary structure of endothelin-1 proposed in the current study is similar to that of Endo et al. [3]. Many similar features include, for example, the helix-like conformation of residues Lys^9–Cys^{11} and a lack of specific interactions between the core and the tail.

While the reason for the difference in the solution conformation of ET-1 reported in these studies [3,4] is unclear, one possibility may be related to the different synthetic routes used in the preparation of the peptides, in particular the use of HgOAc by Saudek et al. [4]. Despite the removal of residual mercuric salts with one equivalent of β-mercaptoethanol in 30% acetic acid following the reaction of the mono-cyclic analog with HgOAc for one hour, it may be tentatively suggested that residual Hg^+ remained associated with endothelin, which has several negatively charged amino acids in the region of Ser^4 to Glu^{10} capable of chelating the metal cation.

Previous structure–activity studies [2] have established the importance of the C-terminal amino acids and the bicyclic structure of ET-1 in determining its biological potency. The current study has established the presence of additional secondary structural motifs including an unusual helical conformation in the region of residues Leu^6–Cys^{15}. The conformation of the C-terminus of ET-1 does not adopt a well defined structure, nor does it appear to interact with the bicyclic portion of the peptide, despite the fact that the terminal tryptophan appears to be crucial for the biological activity of ET-1. We cannot, however, exclude the possibility that when bound to the receptor, additional C-terminal structural elements of ET-1 are populated which are not apparent in the solvent medium described in this report.

REFERENCES

[1] Yanagisawa, M., Kurihara, H., Kimura, S., Tomobe, Y., Kobayashi, M., Mitsui, Y., Yazaki, Y., Goto, K. and Masaki, T. (1988) Nature 332, 411–415.
[2] Kimura, S., Kasuya, T., Sawamura, T., Shinmi, O., Sugita, Y., Yanagisawa, M., Goto, K. and Masaki, T. (1988) Biochem. Biophys. Res. Commun. 156, 1182–1186.
[3] Endo, S., Inoka, H., Ishibashi, Y., Kitada, C., Mizuta, E. and Fujino, M. (1989) FEBS Lett. 257, 149–154.
[4] Saudek, V., Hoflack, J. and Pelton, J.T. (1989) FEBS Lett. 257, 145–148.
[5] Muller, L. and Ernst, R.R. (1979) Mol. Phys. 38, 963–992.
[6] Keeler, J. and Neuhaus, D. (1985) J. Mag. Reson. 63, 454–472.
[7] Braunschweiler, L. and Ernst, R.R. (1983) J. Mag. Reson. 53, 521–528.
[8] Bax, A. and Davis, G. (1985) J. Mag. Reson. 65, 355–360.
[9] Havel, T. (1986) DISGEO: Distance Geometry Program, QCPE Bull. 6, 25.
[10] BIOSYM Technologies, Inc. (San Diego, CA, USA).
[11] Wuthrich, K., Wider, G., Wagner, G. and Braun, W. (1982) J. Mol. Biol. 155, 311–319.
[12] Wuthrich, K. (1986) NMR of Proteins and Nucleic Acids, John Wiley, New York.